

OPTIMIZATION OF HYDROFOIL FOR TIDAL CURRENT TURBINE BASED ON PARTICLE SWARM OPTIMIZATION AND COMPUTATIONAL FLUID DYNAMIC METHOD

by

De-Sheng ZHANG*, Jian CHEN, Wei-Dong SHI, Lei SHI, and Lin-Lin GENG

Research Center of Fluid Machinery Engineering and Technology, Jiangsu University, Zhenjiang,
Jiangsu, China

Original scientific paper
DOI: 10.2298/TSCI1603907Z

Both efficiency and cavitation performance of the hydrofoil are the key technologies to design the tidal current turbine. In this paper, the hydrofoil efficiency and lift coefficient were improved based on particle swarm optimization method and XFOil codes. The cavitation performance of the optimized hydrofoil was also discussed by the computational fluid dynamic. Numerical results show the efficiency of the optimized hydrofoil was improved 11% ranging from the attack angle of 0-7° compared to the original NACA63-818 hydrofoil. The minimum pressure on leading edge of the optimized hydrofoil dropped above 15% at the high attack angle conditions of 10°, 15°, and 20°, respectively, which is benefit for the hydrofoil to avoiding the cavitation.

Key words: tidal current turbine, hydrofoil, particle swarm optimization, cavitation

Introduction

The tidal current turbine [1] is the turbo system that can extract the kinetic energy of tidal and converted it to the mechanical energy. Compare to the wind energy, tidal energy possesses larger energy density which can also offers more predictable and regular renewable energy [2] by the rotation of the blades.

Bahaj *et al.* [3], Batten *et al.* [4], and Bahaj *et al.* [5] investigated the horizontal axis marine (or tidal) current turbine (HATT) based on NACA63-8XX hydrofoil both in cavitation tank and towing tank. Goundar *et al.* [6] studied the hydrofoil used for the HATT, including the NACA63-8XX, NACA00XX, S1020, and HF-Sx. The S814 is proposed by Jo *et al.* [7] to design the HATT which was simulated by the CFD. All of the previous studies focused on the hydro-dynamics of the hydrofoil.

In this paper, Theodorsen transform shape function [8] of the hydrofoil is applied to describe the hydrofoil. The parameters of the shape function are the variables for the optimization program based on the standard particle swarm optimization (PSO) method. Not only the hydrodynamic characteristic of optimized hydrofoil was studied, but also the pressure distributions at the conditions of the high attack angles were investigated. Moreover, compared with the

* Corresponding author; e-mail: zds@ujs.edu.cn

original NACA63-818, the optimized hydrofoil has better hydrodynamic and cavitation characteristics via increasing the min-pressure on the leading edge of the optimized hydrofoil.

The hydrofoil shape function

Theodorsen transform is similar to the Zhukovsky transform [8], which can transform the hydrofoil into the shape function. Next, the transformed shape function is expressed by the Fourier series function. The co-ordinate (x, y) of the hydrofoil decided by eqs. (1) and (2):

$$x = r \frac{a^2}{r} \cos \theta \quad (1)$$

$$y = r \frac{a^2}{r} \sin \theta \quad (2)$$

where θ is the self-varying parameters ranging from 0 to 2π , r is calculated by the transformed shape function, $r = a \exp[\varphi(\theta)]$, in which a is the one quarter of the chord length, and $\varphi(\theta)$ is the determined by eq. (3):

$$\varphi(\theta) = a_1(1 - \cos \theta) + b_1 \sin \theta + a_2(1 - \cos \theta)^2 + b_2 \sin^2 \theta + a_3(1 - \cos \theta)^3 + b_3 \sin^3 \theta \quad (3)$$

where $a_1, a_2, a_3, b_1, b_2,$ and b_3 are the hydrofoil shape function variables.

The max-thickness of the foil is constrained to 18% of the chord length by the XFOIL command test, all of the codes are programmed by the MATLAB software.

The CFD and PSO method

The XFOIL based on the linear vortex theory to calculate the dynamic characteristic of the low speed airfoil including the lift coefficient and lift-to-drag ratio. To validate the predicted results, the numerical simulation method of CFD is used and the basic setting is as followed [9]: the turbulence model is the shear stress transport two equations. The inlet boundary is speed inlet and the velocity, $u = 0.2$ m/s, the outlet boundary is opening. The hydrofoil chord length is 1 m, which corresponds to the $Re = 200000$.

The results of the lift coefficient between the CFD and XFOIL show that the XFOIL software can predict the hydrofoil dynamics with good accuracy at the same Reynolds number (fig. 1) at the low attack angle conditions.

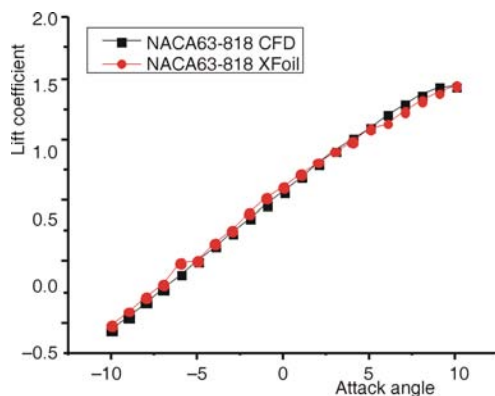


Figure 1. Lift coefficient comparison between CFD and XFOIL

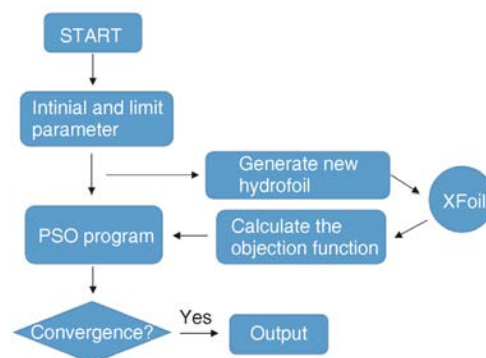


Figure 2. Overall optimization program flowchart

Based on the PSO method [10], the optimization program flowchart is designed as shown in fig. 2. The variable vector has six components, which correspond to the parameters $a_1, a_2, a_3, b_1, b_2,$ and b_3 . The parameters vary from the range from -1 to 1 . Firstly, the variable vector is initiated to $[0, 0, 0.5, 0, 0, 0]$ and the particle start speed is decided by the function rand time 0.5 in the MATLAB. Then, the maximum speed is 0.5 and the minimum speed is -0.5 as well. The PSO evolution equation of particle i are decided:

$$v_{ij}(t+1) = v_{ij}(t) + C_1 r_{1j} [P_{ij}(t) - x_{ij}(t)] + C_2 r_{2j} [P_{ij}(t) - x_{ij}(t)] \quad (4)$$

$$x_{ij}(t+1) = x_{ij}(t) + v_{ij}(t+1) \quad (5)$$

where C_1 and C_2 are the acceleration speed coefficients, both of which are equal to 1.49445 , r_{1j} and r_{2j} are independent random numbers generated by the MATLAB *rand* function, respectively. The weight ratio is set to equal 0.8 finally.

The objection function is shown in eq. (6):

$$f(X) = \frac{0.5}{15} C_L - \frac{0.5}{100} \frac{C_L}{C_D} \quad (6)$$

where C_L and C_D are the lift coefficient and drag coefficient corresponded to the new hydrofoil generated by the parameters $(a_1, a_2, a_3, b_1, b_2,$ and $b_3)$, at the attack angle of six degrees: The objection function is used to describe the new hydrofoil characteristic.

The population size is 15 and max iterations is limited to 1000 . If the program is interrupted, restart the program and set the initial variable vector to the interrupted value. Finally, the optimized hydrofoil is generated with the six components $a_1 = 0.4488, a_2 = -0.1155, a_3 = -0.0313, b_1 = 0.0680, b_2 = -0.1713,$ and $b_3 = 0.0718$.

Results and discussion

The optimized hydrofoil is generated by the parameter function representative of the medium thickness hydrofoil. The max-thickness of the optimized hydrofoil is 18.01% compared to 17.99% of NACA63-818, fig. 3. And the maximum thickness is located 24.7% of chord-length from the leading edge. Also, the maximum camber of the optimized hydrofoil was increased as well as the leading edge radius.

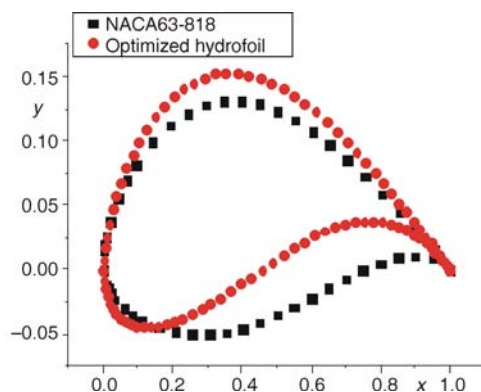


Figure 3. Geometry of the NACA63-818 and optimized hydrofoil

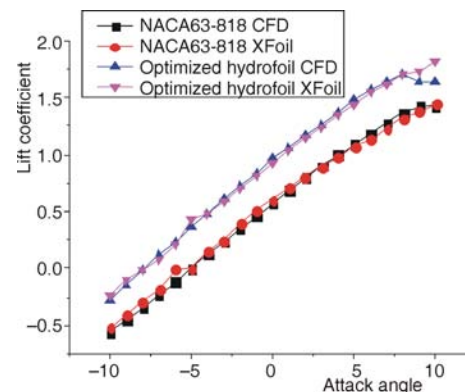


Figure 4. Comparison of lift coefficient predicted by CFD and XFOil

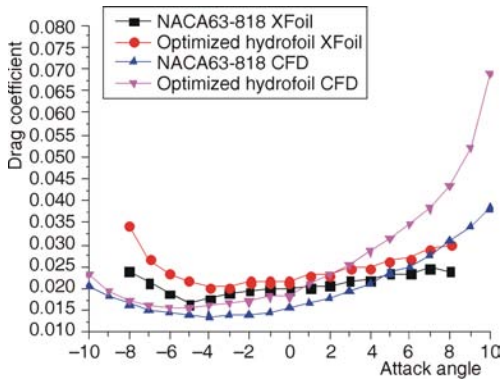


Figure 5. Comparison of drag coefficient t predicted by CFD and Xfoil CFD

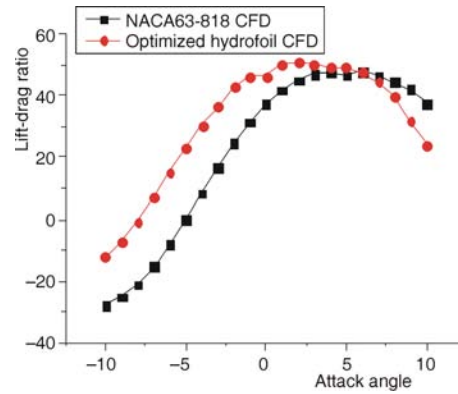


Figure 6. The lift-drag ratio at different attack angle

As shown in figs. 4 and 5, the characteristics of the original NACA63-818 and the optimized hydrofoil were predicted by both Xfoil and CFD. The lift coefficient of the optimized hydrofoil was increased about 0.2 compared to NACA63-818.

Ranging from the 0-6°, the lift-drag ratio simulated by CFD (fig. 6) of the optimized hydrofoil is higher than NACA63-818 hydrofoil. For the design point TSR = 6 the tip speed ration (TSR) is equal to the ratio of blade tip speed to the current speed of the HATT [3], the attack angle of the working blade section mainly locates in the range between 2-5°, where the optimized hydrofoil has larger lift-to-drag ratio obviously.

Due to the HATT is immersed in the water, once the min-pressure of the hydrofoil surface drop to the value below the saturation vapor pressure of water, the cavitation occurs, which may result in the blade damage of the HATT as shown in fig. 7. As we know, the cavitation can

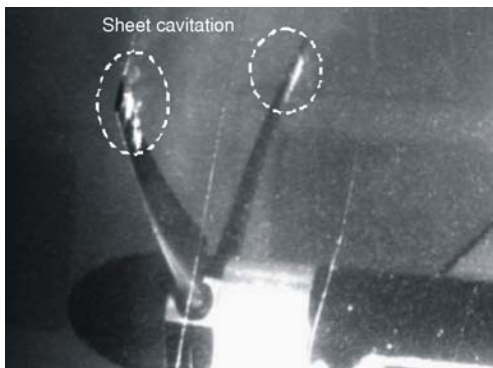


Figure 7. Cavitation occur in the low pressure area

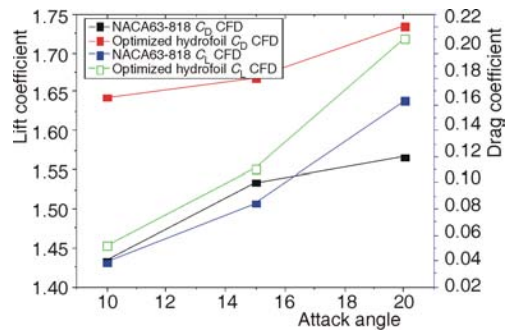


Figure 8. The hydrofoil characteristic at high attack angle

be avoided by improving the minimum pressure on the hydrofoil. The hydrodynamics of the optimized hydrofoil and NACA63-818 hydrofoil are also studied to discuss the cavitation performance as shown in fig. 8 using Xfoil codes and CFD method.

The high attack angles often operate at the off-design conditions, and the hydrofoil lift and drag coefficient as well as the minimum pressure of the hydrofoil should be considered. In

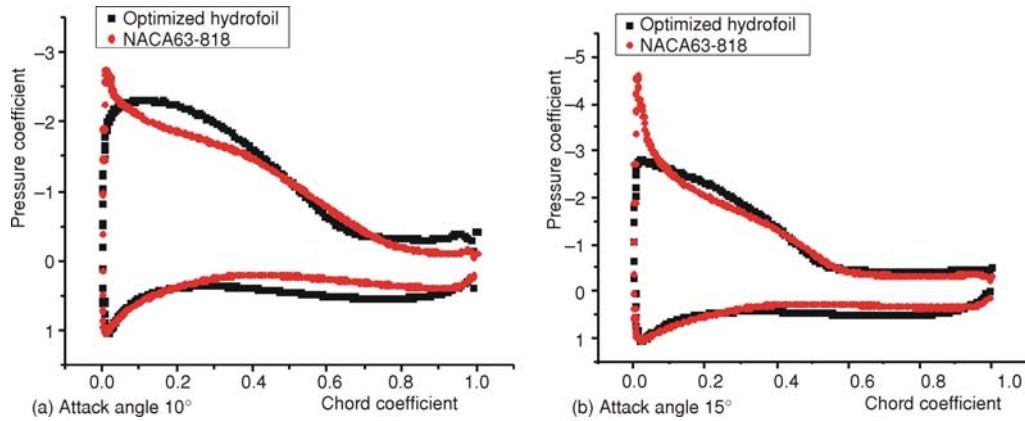


Figure 9. Pressure coefficient distribution along the chord length

order to protect the HATT blade from the cavitation damage, the minimum pressure of the hydrofoil should be taken into account. Both the optimized hydrofoil and NACA63-818 hydrofoil were simulated at attack angle of 10°, 15° (fig. 9), and 20°. The lift coefficient of the optimized hydrofoil is larger than NACA63-818 hydrofoil, and the drag coefficient is also increased owing to the hydrofoil stall. The reason is that the optimized hydrofoil has higher max-camber which blocks the fluid. Compared to the efficiency of the HATT system, the stability and safety at the off-design condition should be taken into account.

The pressure coefficient distributions simulated by CFD along the chord length are presented at various large attack angles as shown in fig. 9. The results show that the values of the minimum pressure of the optimized hydrofoil were increased at the large attack angle conditions. Figure 9(a) shows that the minimum pressure coefficient of the NACA63-818 and the optimized hydrofoil are -2.7 and -2.3, respectively, at the attack angle of 10°. Also, in fig. 9(b), when the attack angle is increased to 15°, the minimum pressure coefficient is dropped to -4.7 and -2.7. At the attack angle of 20°, the minimum pressure coefficient of the NACA63-818 and the optimized hydrofoil decrease to -6.3 and -3.8. Compared the NACA63-818 and the optimized hydrofoil, as shown in fig.10, the low pressure of NACA 63-818 (right) in the area A, B, and C is obviously larger than the optimized hydrofoil (left).

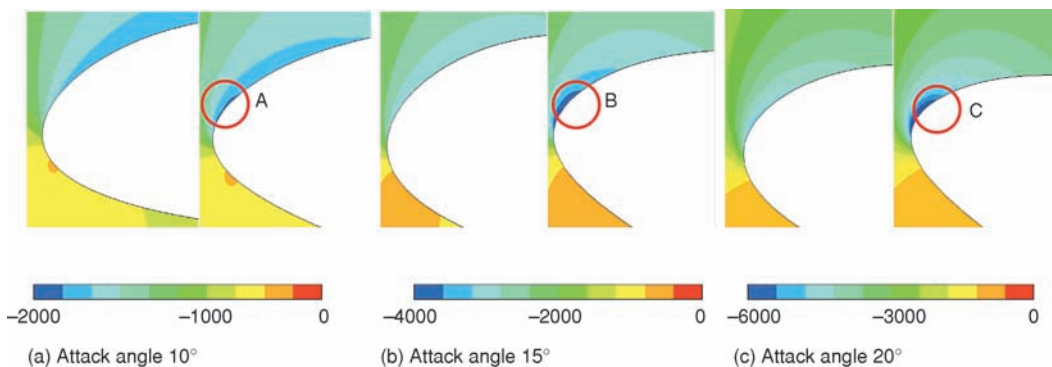


Figure 10. Pressure distributions near the leading edge of hydrofoil
 (for color image see journal web site)

Conclusion

An improved hydrofoil based on the PSO method and Theodorsen transformation is proposed in this paper. Compared to the original NACA63-818, the lift coefficient of optimized hydrofoil was improved obviously as well as the lift-drag ratio at the design attack angle condition. And at off-design operating conditions, the optimized hydrofoil with higher max-camber and larger leading edge radius gets the better cavitation performance via increasing the hydrofoil minimum pressure as well as narrow the low pressure region, which is available to avoiding the cavitation inception of the HATT at the off-design conditions.

Acknowledgment

This work was supported by National Natural Science Foundation of China (Grant No. 51479083), Prospective joint research project of Jiangsu Province (Grant No. BY2015064-08), Key Research & Design programs of Jiangsu Province (Grant No. BE2015146 and BE2015001-3) and PAPD.

Reference

- [1] Masters, I., Orme, J., Tidal Current Turbine, patents No. CA2649828 A1, 2007
- [2] Liu, L. Q., et al., The Development and Application Practice of Neglected Tidal Energy in China, *Renewable & Sustainable Energy Reviews*, 15 (2011), 2, 1089-1097
- [3] Bahaj, A. S., et al., Experimental Verifications of Numerical Predictions for the Hydrodynamic Performance of Horizontal Axis Marine Current Turbines, *Renewable Energy*, 32 (2007), 15, pp.2479-2490
- [4] Batten, W. M. J., et al., The Prediction of the Hydrodynamic Performance of Marine Current Turbines, *Renewable Energy*, 33 (2008), 5, pp.1085-1096
- [5] Bahaj, A. S., et al., Power and Thrust Measurements of Marine Current Turbines under Various Hydrodynamic Flow Conditions in a Cavitation Tunnel and a Towing Tank, *Renewable Energy*, 32 (2007), 3, pp. 407-426
- [6] Goundar, J. N., et al., Numerical and Experimental Studies on Hydrofoils for Marine Current Turbines, *Renewable Energy*, 42 (2012), 1, pp.173-179
- [7] Jo, C. H., et al., Performance of Horizontal Axis Tidal Current Turbine by Blade Configuration, *Renewable Energy*, 42 (2012), 1, pp.195-206
- [8] Drela, M., XFOIL: An Analysis and Design System for Low Reynolds Number Airfoils, *Low Reynolds Number Aerodynamics*, Springer Berlin Heidelberg, 54 (1989), pp. 1-12
- [9] Luo, X. Q., et al., Multi-Point Design Optimization of Hydrofoil for Marine Current Turbine, *Journal of Hydrodynamics*, 26 (2014), 5, pp. 807-817
- [10] Kennedy, J., Welcome to this Special Issue on Particle Swarms, *International Journal of Computational Intelligence Research*, 4 (2008), 2, p. 1